DOI: 10.1002/chem.201103235

Is Our Way of Thinking about Excited States Correct? Time-Resolved Dispersive IR Study on *p*-Nitroaniline

Sudhakar Narra, Shu-Wei Chang, Henryk A. Witek, and Shinsuke Shigeto*[a]

Abstract: Low-lying excited electronic states of an important class of molecules known as push–pull chromophores are central to understanding their potential nonlinear optical properties. Here we report that a combination of high-sensitivity nanosecond time-resolved dispersive IR spectroscopy and DFT calculations on *p*-nitroaniline (PNA), a prototypical push–pull molecule, reveals that PNA in the lowest excited triplet state has a partial quinoid structure. In this structure, the quinoid configuration is restricted to a part of the phenyl ring adjacent to the NO_2 group. The partial quinoid structure of PNA cannot be explained by a commonly used hybrid of a neutral form and a zwitterionic charge-transfer form. Our findings not only cast doubt on the general applicability of the classical way of looking at excited states, based exclusively on characteristic resonance structures, but also provide deeper insights into excited-state structure of highly polarizable molecular systems.

Keywords: density functional calculations · excited states · IR spectroscopy · push–pull chromophores · time-resolved spectroscopy

Introduction

Valence-bond resonance structures are a simple but intuitive concept that is commonly used in various branches of chemistry. They are hypothetical formulae representing electronic structure of molecules in an approximate fashion; an actual representation should be thought of as a linear combination of all conceivable resonance structures that can be written for a given molecule. Organic chemists often use resonances structures to provide a qualitative account of chemical structures and reactivities. Resonance structures have been applied to describe electronic structures of molecules not only in the ground state,[1–3] but also in electronic excited states. For example, excited states of an interesting class of molecules known as push–pull chromophores, in which an electron-donating group and an electron-withdrawing group are linked by a conjugated system, have been understood in terms of a mixture of neutral and charge-transfer (CT) resonance structures.[4] Herein, we use a combination of nanosecond time-resolved dispersive IR spectroscopy and DFT to demonstrate that the electronic structure of the lowest excited triplet (T_1) state of *p*-nitroaniline (PNA) in acetonitrile (ACN) is accounted for not by a commonly used hybrid of neutral form **1** and zwitterionic form **2**, but by an unusual structure similar to **3**, in which a quinoid structure is restricted to a part of the phenyl ring in the vicinity of the NO_2 group (Figure 1). This finding shows that our usual way of thinking about excited states of push–pull molecules can be erroneous, and lead to dubious predictions and intuitions.

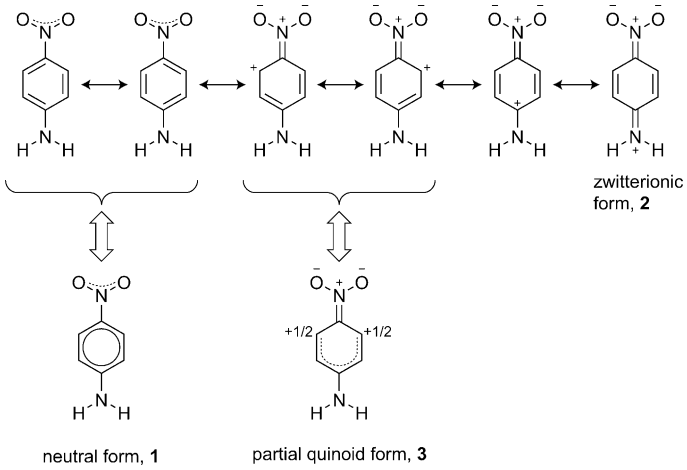

Figure 1. Representative resonance structures of PNA and their hybrids: neutral form **1**, zwitterionic form **2**, and partial quinoid form **3**.

p-Nitroaniline is a prototypical push–pull molecule exhibiting a large first hyperpolarizability[5–11] and nonlinear optical properties with possible applications for electrooptic and second-harmonic generation materials. As a model system, PNA has long been studied both experimentally[4,12–22] and theoretically.[23–27] A number of ultrafast spectroscopic studies[28–31] have been done to understand the dynamics of PNA after photoexcitation. The lowest excited singlet (S_1) state of PNA is well-known to have CT character with a large dipole moment[27] of about 15 D, and the S_1 state undergoes very

[a] S. Narra, S.-W. Chang, Prof. Dr. H. A. Witek, Prof. Dr. S. Shigeto
Department of Applied Chemistry and Institute of Molecular Science
National Chiao Tung University
1001 Ta-Hsueh Road, Hsinchu 30010 (Taiwan)
Fax: (+886) 3-5723764
E-mail: shigeto@mail.nctu.edu.tw

Supporting information for this article is available on the WWW under http://dx.doi.org/10.1002/chem.201103235.

rapid (< 0.3 ps) nonradiative relaxation to the ground (S_0) state by internal conversion (IC) or to the triplet manifold by intersystem crossing (ISC).[29,31] In a conventional two-state valence-bond model, the ground state is dominated by neutral form **1**, whereas the S_1 state has a considerable contribution of zwitterionic form **2**, which explains the large change in dipole moment from about 6 D in the ground state[32] to about 15 D in the S_1 state.[27]

In light of the fact that the T_1 state is a primary channel for the photophysical and photochemical processes in the nanosecond to microsecond time region, it is desirable to obtain detailed molecular information on this state as well. Schuddeboom et al.[30] used time-resolved microwave conductivity to determine the lifetime and dipole moment of the T_1 state in benzene and dioxane. It was shown that the dipole moment of T_1 PNA is in the range of 9–11 D, depending on the solvent and the ISC quantum yield.[30] Thomsen and co-workers[31] measured the transient absorption spectrum in the 340–960 nm range of PNA excited at 400 nm, which is assigned to vibrationally hot PNA molecules in the ground state and triplet–triplet absorption bands. A theoretical investigation was also performed recently by Kosenkov and Slipchenko,[25] who predicted that the lowest bright triplet state (1^3A_1) has a much smaller dipole moment (8.7 D) than the CT singlet state (12.9 D). Although it would be reasonable to explain these observations on the basis of the two-state model by assuming that the T_1 state of PNA has a CT structure[33] analogous to the S_1 state, this analogy needs to be critically tested by more direct information on the bonding structure of PNA in the T_1 state. Vibrational spectroscopy is undoubtedly a powerful approach that permits one to access such information. Here we aim to provide new insights into the electronic and molecular structure of T_1 PNA on the basis of experimental and theoretical IR spectra, which will call into question the applicability of the classical resonance-structure picture for elucidation of the electronic structure of excited states of molecules.

Results and Discussion

Time-resolved IR study: First, we present experimental data obtained by time-resolved IR spectroscopy (see Experimental Section for details) of PNA in CD_3CN, with a focus on characterization of the triplet-state IR spectra of PNA and its isotopomers. Figure 2 displays the time-resolved IR difference spectra of PNA in argon-saturated CD_3CN solution, together with the ground-state (S_0 PNA) spectrum recorded with the dispersive spectrometer. The ground-state spectrum of PNA (Figure 2a) shows four principal IR bands peaking at 1317, 1503, 1600, and 1636 cm^{-1}. The 1317 cm^{-1} band is accompanied by a shoulder at 1332 cm^{-1}. The peak positions are in good agreement with the literature.[17,24] Our DFT calculations (see below) reveal that these four bands are attributed predominantly to the NO_2 symmetric stretch, NO_2 antisymmetric stretch, and admixtures of NH_2 scissoring and the C–C stretch, respectively. In the time-resolved IR difference spectra of PNA in CD_3CN (Figure 2b), three positive peaks at 1250, 1480, and 1605 cm^{-1} and four negative peaks at the same positions as in Figure 2a are observed. The positive peaks correspond to the transient absorption of photogenerated molecular species, and the negative peaks to depletion (bleaching) of the ground-state population of PNA. The transient absorption arises instantaneously and decays away within a few microseconds, synchronously with recovery of the ground-state depletion. Little bleaching signal remains in the 7.0–8.0 μs spectrum. Previous transient absorption studies[29–31] revealed that relaxation of the S_1 state of PNA proceeds extremely rapidly to S_0 by IC or to T_1 by ISC. The time constants for IC and ISC of PNA in water are 250 fs[29] and 10 ps,[31] respectively. These timescales are much faster than the time resolution of our apparatus, so the dynamics involving the S_1 state is completely over within one laser pulse in our experiment. Therefore, we assign the transient species detected here to PNA in the T_1 state, which is generated from S_1 as a result of ISC.

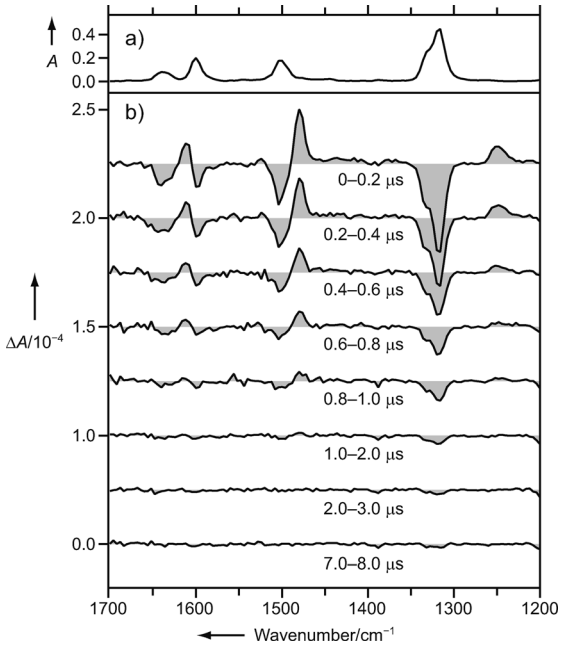

Figure 2. a) Ground-state IR spectrum and b) time-resolved IR difference spectra of PNA in CD_3CN (0.25 mM) excited at 355 nm with argon bubbling. Each time-resolved spectrum is offset by 5×10^{-5} for clarity of display.

To corroborate our interpretation, we performed a singular value decomposition (SVD) analysis of the time-resolved IR spectra, which shows that the observed dynamics can be reproduced by considering a single independent component. The intrinsic spectrum of the component (Figure S1a in the Supporting Information) is essentially identical to the 0–0.2 μs spectrum (Figure 2b) and decays with an exponential time constant of 430 ns (Figure S1b in the Supporting Information). This time constant is consistent with the reported lifetime of T_1 PNA (434 ns in ACN[22] and 275 ns in dioxane[30]).

Further support comes from oxygen-quenching effects on the transient absorption of PNA. As shown in Figure S2a in the Supporting Information, the intensity of the transient absorption bands decreases due to oxygen bubbling and decays much faster than with argon bubbling. Even the strongest positive band at 1480 cm^{-1} completely disappears already 200 ns after photoexcitation. To examine the quenching effects on the kinetics, we compared the time profiles of the intensity at 1250 cm^{-1} between argon- and oxygen-bubbling measurements (Figure S2b in the Supporting Information). The exponential time constant is reduced by 75% with oxygen bubbling. The accumulated experimental evidence leads us to the conclusion that the dynamics we have observed (Figure 2b) is attributed to formation of the triplet state of PNA and its subsequent relaxation back to the ground state. Note that, even in the absence of oxygen, T_1 PNA seems to show self-quenching effects at higher concentrations of PNA, possibly resulting in the formation of PNA oligomers.[22,30] We did find that at 1 mM, only about 80% of the excited PNA molecules eventually return to the ground state. In contrast, at 0.25 mM, little bleaching signal remains after the decay of T_1 PNA completes.

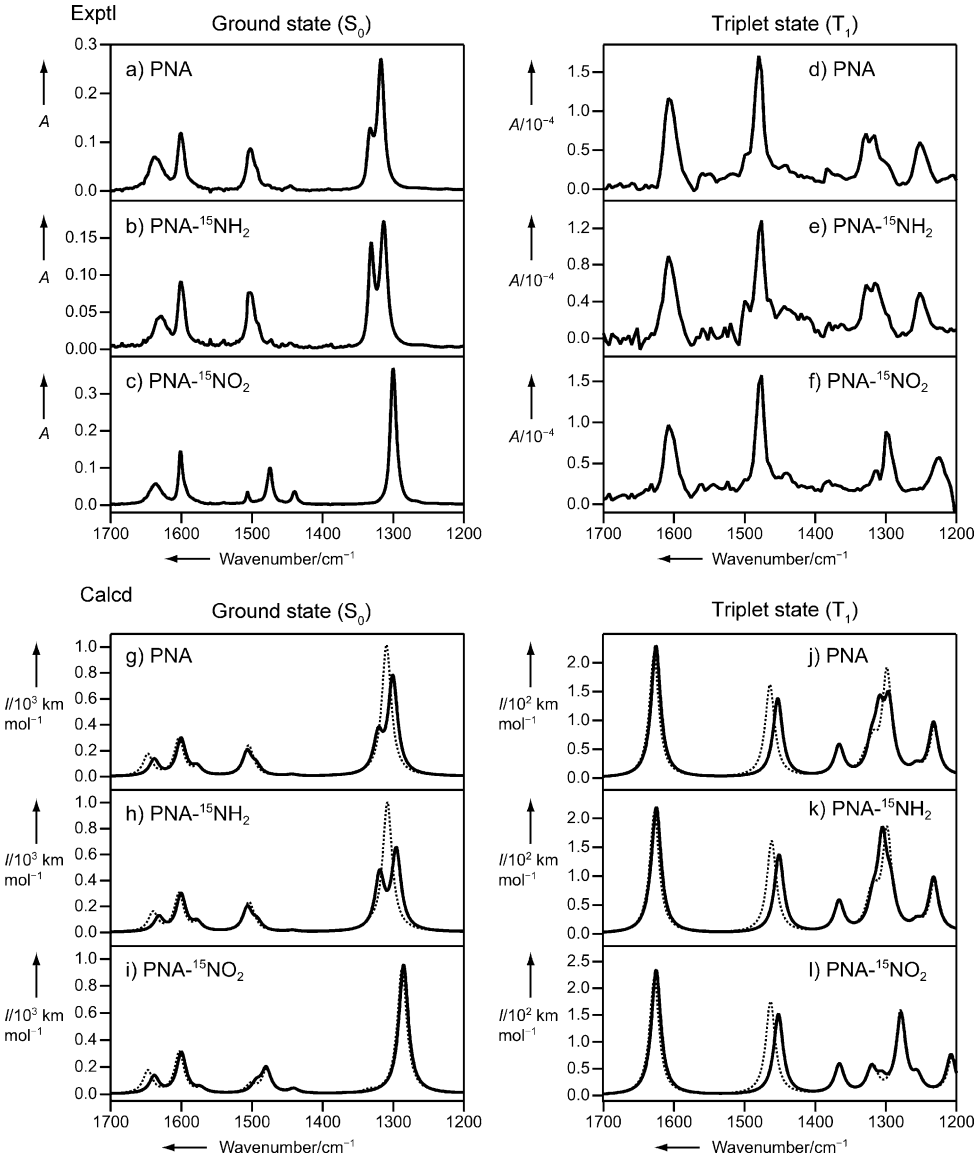

Figure 3. Upper panels: experimental IR spectra of PNA and its isotopomers, PNA-$^{15}NH_2$ and PNA-$^{15}NO_2$. a–c) Ground-state (S_0) spectra recorded with an FTIR spectrometer. d–f) Lowest excited triplet-state (T_1) spectra obtained by compensating the depletion of the ground-state absorption. Lower panels: IR spectra of PNA, PNA-$^{15}NH_2$, and PNA-$^{15}NO_2$ calculated by using the PNA+2ACN model with (solid line) and without (dotted line) elongation of the C–NH_2 bond by 0.012 Å. g–i) The ground state. j–l) The T_1 state. See text for details.

The observed positive peaks have been identified as originating from PNA in the T_1 state. The true triplet-state spectrum of PNA can be determined by adding an appropriately weighted ground-state spectrum to the difference spectrum so that the negative peaks would be compensated.[34,35] The IR spectrum of T_1 PNA obtained with such a compensation procedure is presented in Figure 3. The IR spectra of PNA-$^{15}NH_2$ and PNA-$^{15}NO_2$ in the T_1 state derived in a similar manner are also shown in Figure 3, together with their ground-state FTIR spectra. The vibrational frequencies determined for all three compounds are listed in Table 1. The experimental isotope-substitution effects are summarized as follows. The ^{15}N substitution in the NH_2 group does not affect much the recorded ground- and triplet-state IR spectra, except for modified frequency spacing between the doublet components of the 1317 cm^{-1} band (compare Figure 3a and b for S_0 and Figure 3d and e for T_1). In contrast, ^{15}N substitution in the NO_2 group alters the spectral pattern in the 1420–1520 cm^{-1} region and the doublet at 1317 and 1332 cm^{-1} for S_0 PNA (Figure 3c), and shifts the 1250 cm^{-1} band by −25 cm^{-1} for T_1 PNA (Figure 3f).

Theoretical IR spectra: We now attempt to provide a theoretical interpretation for the experimentally recorded IR spectrum of T_1 PNA. We are aware that modeling IR spectra in solution phase requires in general a time-dependent investigation of dynamics of an ensemble of PNA/ACN mol-

Table 1. Experimental and calculated vibrational frequencies and assignments of major IR bands (1200–1700 cm^{-1}) of PNA, PNA-$^{15}NH_2$, and PNA-$^{15}NO_2$ in the ground state and the lowest excited triplet state.

Experiment[a]			DFT calculation[b]			Assignment[c]
PNA	PNA-$^{15}NH_2$	PNA-$^{15}NO_2$	PNA	PNA-$^{15}NH_2$	PNA-$^{15}NO_2$	(approximate description)
ground (S_0) state						
1636	1630	1637	1638	1632	1638	$\delta_s(NH_2$ scissoring)
1600	1600	1601	1600	1600	1600	ν(C–C), $\delta_s(NH_2$ scissoring)
			1578	1577	1573	ν(C–C), $\nu_{as}(NO_2)$, $\rho(NH_2)$
1503	1503	1475	1507	1506	1480	$\nu_{as}(NO_2)$, ν(C–C)
1494	1494	1506	1494	1492	1494	δ(C–H), ν(C–C), ν(C–NH_2), $\delta_s(NH_2$ scissoring)
		1475				
1332	1331		1321	1319	1313	$\nu_s(NO_2)$, δ(C-H), out-of-phase combination of ν(C-NH_2) and ν(C-NO_2)
1317	1314	1300	1300	1296	1285	$\nu_s(NO_2)$, δ(C-H), in-phase combination of ν(C-NH_2) and ν(C-NO_2)
triplet (T_1) state						
1605	1606	1605	1626	1624	1625	$\delta_s(NH_2$ scissoring), ν(C-C)
1480	1476	1478	1453	1451	1452	δ(C–H), ν(C–C), ν(C–NH_2), $\delta_s(NH_2$ scissoring)
			1366	1366	1366	ν(C–C), $\rho(NH_2)$
			1320	1319	1320	
≈1320	≈1320	≈1300	1309	1305	1306	$\nu_s(NO_2)$, δ(C–H), in-phase combination of ν(C–NH_2) and ν(C-NO_2)
			1296	1293	1279	$\nu_s(NO_2)$, δ(C–H), out-of-phase combination of ν(C–NH_2) and ν(C–NO_2)
			1257	1256	1255	
1250	1250	1225	1232	1232	1207	$\nu_{as}(NO_2)$, ν(C–C), $\rho(NH_2)$

[a] Taken from FTIR spectra for S_0. [b] B3LYP/PNA+2ACN with slight elongation (0.012 Å) of the C–NH_2 distance. Scaling factor = 0.972. [c] ν: stretching; δ: in-plane bending; ρ: rocking.

ecules at some finite temperature. An appropriate study would consist of running a molecular dynamics trajectory for such an ensemble and obtaining the IR spectrum via the Fourier transform of the recorded dipole moment autocorrelation function. Unfortunately, at the present level of development of computational methods, such a study is not practically feasible, in particular for molecules in excited states. Instead, we chose to employ traditional, time-independent instruments of quantum chemistry, namely, DFT with the B3LYP exchange correlation functional (see Experimental Section for details).

Another important issue here is a careful choice of an appropriate molecular model. Usually, for the interpretation of IR spectra of molecules in the liquid phase, the calculations are performed for a single gas-phase molecule, under the assumption that there is no pronounced difference between the spectra of gas-phase and solvated molecules. Here we can test this supposition by studying the ground state of PNA in detail, because accurate experimental data are readily available for the ground state. After finding a molecular model capable of reproducing the observed ground-state spectra of PNA and its isotopomers in a satisfactory manner, we proceeded to interpret the triplet-state IR spectrum of PNA.

The calculated gas-phase IR spectrum of PNA (Figure 4b) is in apparent contrast with the experimental result

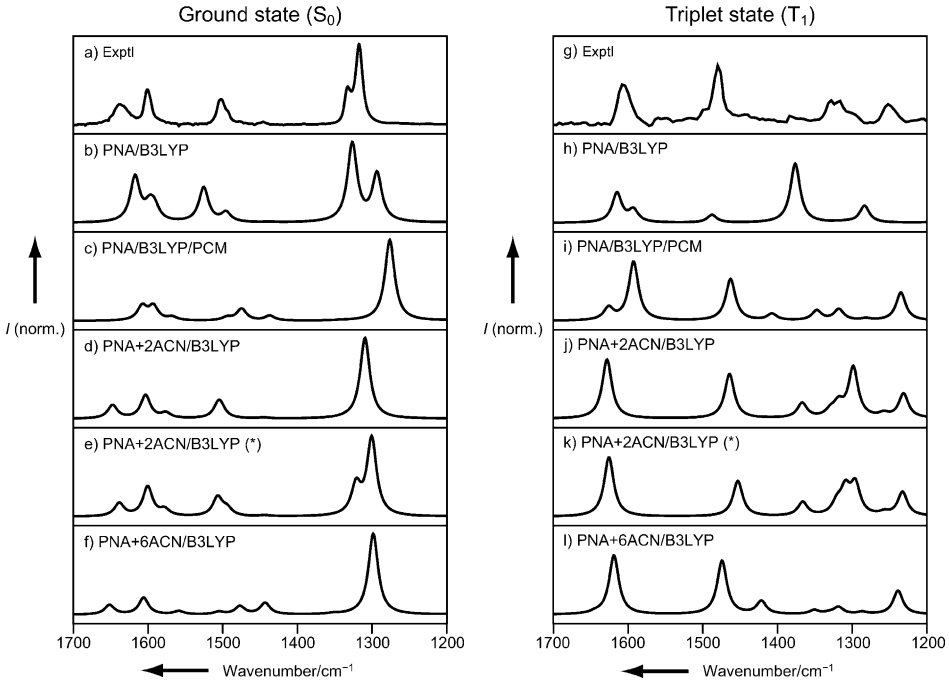

Figure 4. Comparison of experimental and calculated DFT/B3LYP IR spectra of PNA in the ground state (left panel) and in the lowest excited triplet state (right panel). a,g) Experimentally recorded IR spectra of PNA in CD_3CN (0.25 mM). b,h) A gas-phase molecular model. c,i) PCM model. d,j) Explicitly solvated model with two CD_3CN molecules attached to the NH_2 group (PNA+2ACN model). e,k) PNA+2ACN model with slight elongation (0.012 Å) of the C–NH_2 bond. f,l) Explicitly solvated model with six CD_3CN molecules (PNA+6ACN).

(Figure 4a). First, the 1250–1370 cm^{-1} region displays two, well-separated strong bands with reversed relative intensities. In addition, the 1450–1650 cm^{-1} region is distinct from the experiment. These findings suggest that solvation of PNA by CD_3CN has substantial effects on the resulting IR spectra and that one should not use a bare, gas-phase molecular model for interpretation of the triplet-state IR spectrum. It is customary to account for the solvent effects by using some implicitly solvated model, in which the solvent is represented, for example, as a dielectric continuum with a given dielectric constant ($\varepsilon = 37.5$ for CD_3CN). The resulting spectrum obtained with B3LYP combined with the polarizable continuum model (PCM) does not show any considerable improvement in comparison with the gas-phase spectrum. The main difference from experiment for the simulated B3LYP/PCM IR spectrum of PNA (Figure 4c) concerns three details: 1) the doublet structure in the 1317 cm^{-1} band is missing, 2) the band around 1600 cm^{-1} is split, and 3) the band at 1636 cm^{-1} is missing. The overall comparison of the computed gas-phase and PCM spectra with experiment suggest that none of these methods can be successfully used for interpretation of the recorded triplet-state IR spectrum of PNA.

Fortunately, the problems with the IR spectra obtained with the gas-phase and PCM approaches can be almost completely resolved if one employs an explicitly solvated model of PNA in which two CD_3CN molecules are hydrogen-bonded to the NH_2 group (hereafter referred to as the PNA + 2 ACN model; see Figure S3a in the Supporting Information for its geometry). The resulting spectrum (Figure 4d) shows very good agreement with the experimental data, except for the missing hump at 1332 cm^{-1}. We considered a multitude of various explicitly solvated models containing one to six CD_3CN molecules attached either to the NH_2 group or the NO_2 group, or aligned along the ring (see Figure 4f for the calculated IR spectrum and Figure S3b in the Supporting Information for the geometry of six solvent molecules, i.e., PNA + 6 ACN). All of the resulting spectra are quite similar in terms of a strong single band in the 1300–1400 cm^{-1} region and reasonable agreement with experiment in the 1600–1700 cm^{-1} region. The main difference lies in the region around 1500 cm^{-1}, for which the presence of four or more solvent molecules results in two split bands. This is an interesting finding, possibly suggesting that the first solvation shell of PNA consists of maximally three solvent molecules. One may argue that PNA is capable of forming only two hydrogen bonds with the solvent molecules through the NH_2 group. However, we have found that B3LYP predicts binding energies of CD_3CN to the NH_2 and NO_2 groups of similar order of magnitude: 5.5 and 3.5 kcal mol^{-1}, respectively.

The optimized structures of PNA with explicitly attached solvent molecules display small variations in equilibrium geometry, which concern mainly the out-of-plane angles of the NH_2 and NO_2 groups and the C–NH_2 and C–NO_2 distances. We have anticipated that the dependence of the out-of-plane, low-frequency motions of the NH_2 and NO_2 groups can have substantial influence on the simulated IR spectra.[28] It turned out that this effect is negligible,[4,16] but in the course of this investigation, we have found that some part of the spectrum changes quite dramatically with variation of the C–NH_2 distance. Slight elongation (0.012 Å) of the C–NH_2 bond from its equilibrium length (1.352 Å) produces a hump on the single band at 1300 cm^{-1}, and gives perfect agreement between the simulated spectra and the experimental results in the whole spectral window studied (Figures 3g and 4e). The energy of 0.07 kcal mol^{-1} associated with such elongation is completely negligible on the molecular scale.

The origin of the doublet feature at around 1320 cm^{-1} has been a subject of debate.[13–15,17,19,21] Two possible mechanisms for this doublet have been suggested: one is a Fermi resonance[13,17] and the other is the existence of two distinct solvated forms of PNA.[14,21] However, according to our calculations, the higher- and lower-wavenumber components of the doublet are attributed to the NO_2 symmetric stretch coupled with out-of-phase and in-phase combinations of the C–NH_2 and C–NO_2 stretches, respectively (see Table 1). We have found that their relative IR intensities are profoundly affected by the geometry of PNA as well as by explicit solvation.

One may argue that the bond elongation we have devised is not justified. However, we would like to present a number of justifications for such an action. First, we note that the computed C–NH_2 bond length in the free and solvated PNA models varies between 1.343 and 1.375 Å depending on the number and orientation of the explicitly attached solvent molecules. The elongation we engineered to reproduce the experimental spectrum yields a bond length of 1.364 Å, which falls in the above-mentioned interval. Note that the engineered elongation is comparable in magnitude to a typical error (approximately 0.01 Å) expected from DFT calculations of equilibrium bond lengths. The elongation may give rise to a certain intensity redistribution in the simulated IR spectrum, but it does not influence the positions of the vibrational bands. If we reoptimize the molecular geometry while keeping the new C–NH_2 bond length frozen and recalculate the spectrum, the largest frequency change is only 15 cm^{-1}. One may inquire whether the engineered elongation has some physical interpretation. This question is readily answered by taking into account the contrast between the intrinsic static nature of the model used in our quantum chemical calculations and the inherently dynamic behavior of a real vibrating molecule. Quantum chemical methods usually give us information about the (static) equilibrium bond lengths r_e, but it would be more desirable to consider the distances averaged over the ground vibrational wave functions r_0, which provide more physically meaningful information about the time-averaged interatomic distances in a molecule. For a purely harmonic vibration, these two quantities would be equal. However, the C–NH_2 bond stretch, like nearly any other stretching vibration, has an anharmonic vibrational potential for which r_0 is larger than r_e. Additional support for the C–NH_2 bond elongation comes

from the simulated IR spectra of PNA-$^{15}NH_2$ and PNA-$^{15}NO_2$. The PNA+2 ACN model (dotted line, lower left panel of Figure 3) correctly predicts the isotope-substitution effects in the NO_2 group but fails to predict the distinct doublet structure of the 1317 cm^{-1} band. In contrast, the PNA+2 ACN model with slightly elongated C–NH_2 bond (solid line, lower left panel of Figure 3) correctly predicts the isotope substitution effects in both NH_2 and NO_2 groups.

We have demonstrated above that the PNA+2 ACN model with slightly elongated C–NH_2 bond is capable of reproducing all the accumulated spectral evidence for the ground state of PNA. We are therefore ready to interpret the IR spectrum of the T_1 state of PNA shown in Figure 3d. The experiment detects four principal bands in the triplet-state spectrum at 1250, 1320, 1480, and 1605 cm^{-1}. The engineered PNA+2 ACN model (Figure 3j) closely resembles this experimental pattern by reproducing these bands at 1232, 1309, 1453, and 1626 cm^{-1}, respectively. The assignments of these bands are as follows. The band at 1232 cm^{-1} corresponds predominantly to the NO_2 antisymmetric stretch. The intense composite band at 1309 cm^{-1} has a complicated vibrational composition, namely, a mixture of in-plane C–H bending, C–NH_2 and C–NO_2 stretches, C–C stretch, and NO_2 symmetric stretch. The band at 1453 cm^{-1} is a mixture of in-plane C–H bending and C–NH_2 and C–NO_2 stretches. The band at 1626 cm^{-1} originates from a mixture of the NH_2 scissoring motion and C–C stretch. An analogous band appears in the IR spectrum of the ground state at 1636 cm^{-1}, although with much lower intensity. As can be seen from Figure 3d–f and j–l, the PNA+2 ACN model with slightly elongated C–NH_2 bond again does an excellent job of reproducing the experimental triplet-state IR spectra of all three isotopomers. The frequencies and assignments of T_1 PNA vibrations derived from our calculations are summarized in Table 1. The shift of the IR bands on going from S_0 to T_1 revealed by our calculations can be easily seen in Figure S4 in the Supporting Information.

Photoexcitation of PNA to the S_1 state has been interpreted in terms of CT from the electron-donating NH_2 group to the electron-withdrawing NO_2 group (zwitterionic form **2**).[4,27–31] It would be natural to expect that the T_1 state would be of similar character as well. However, our interpretation of the IR spectra of S_0 and T_1 PNA does not fully confirm this hypothesis. No significant change in vibrational frequencies associated with the NH_2 group (only −80 cm^{-1}) with a simultaneous large frequency shift in the NO_2 antisymmetric stretch (−270 cm^{-1}) suggests that the excitation is rather local and occurs only at the NO_2 moiety. It is relatively easy to design a local molecular orbital picture of the $T_1 \leftarrow S_0$ excitation. In the ground state, the four π-electrons of the NO_2 moiety display the $\pi^2\pi^{\bigcirc 2}\pi^{*0}$ configuration, which is changed to $\pi^2\pi^{\bigcirc 1}\pi^{*1}$ upon excitation. Such a change leads to a reduction of the N–O bond order from approximately 1.5 in the ground state to 1.25 in the T_1 state. This change can be observed in a twofold way: vibrational frequencies and bond lengths. The typical frequency of the NO_2 antisymmetric stretch of order 1.5 is expected to be about 1550 cm^{-1}, whereas the single N–O bond stretch of oximes usually appears around 940 cm^{-1}. In our calculations, the frequency associated with the NO_2 antisymmetric stretch is reduced from 1507 cm^{-1} in the S_0 state to 1232 cm^{-1} in the T_1 state. The typical length of the N=O bond is approximately 1.2 Å, whereas that of a single bond is 1.4 Å. As shown in Figure 5, our simulations reveal N–O bond lengths

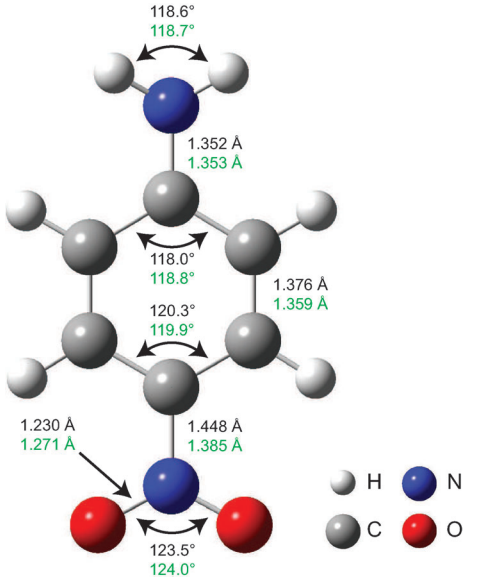

Figure 5. Bond lengths and angles in the S_0 state (upper value) and T_1 state (lower value in green) derived from the DFT calculations with the PNA+2 ACN model.

of 1.230 Å in the S_0 state and 1.271 Å in the T_1 state. Both observations support the local character of the $T_1 \leftarrow S_0$ excitation. The local excitation mechanism described here is further confirmed by the shortening of the C–NO_2 bond upon excitation (1.448→1.385 Å), which is associated with the contribution of the single π* electron localized on the nitrogen atom to the aromatic ring. Such a contribution leads to a partial quinoid structure of PNA in the T_1 state. Note that the picture obtained here is quite different from that given by conventional hybrids of resonance structures such as **1** and **2** in organic chemistry.[3,4] The quinoid structure is actually restricted only to the part of the ring in the vicinity of the NO_2 moiety, because the C–NH_2 bond length is practically identical between the two electronic states (1.352 vs. 1.353 Å, Figure 5). If we are compelled to translate this partial quinoid structure into the language of resonance structures, we may find that **3** would be the closest with formal charges of $+^1/_2$ at the *ortho* positions to the NO_2 group. It is also consistent with the experimental evidence[30] that the T_1 state shows a less pronounced CT character compared to the S_1 state.

Conclusion

The experimental and theoretical evidence presented here strongly suggests that the T_1 state of PNA has a partial quinoid structure, which is in apparent contrast with the conventional two-state models describing excited states of push–pull compounds. Such a partial quinoid structure may also be found for other push–pull compounds in excited states. *p*-Dimethylaminobenzonitrile (DMABN) is one of the most extensively studied compounds of this kind. A number of time-resolved IR[36–39] and Raman[40,41] studies have been performed to elucidate the CT S_1 and T_1 states of DMABN, and provide conclusive evidence for a long-standing controversy[42] as to whether the S_1 state has a twisted intramolecular CT (TICT) or planar CT structure. With respect to the T_1 state, Hashimoto and Hamaguchi[36] suggested the presence of the TICT T_1 state. In contrast, Ma et al.[40] reported that T_1 DMABN has a planar or nearly planar structure with high negative charge localized on the C≡N group and conjugation between the ring and the N-$(CH_3)_2$ group. Our results demonstrate that a combination of time-resolved IR spectroscopy and the DFT/B3LYP method with the engineered explicit solvation model can be helpful to resolve the long-standing issue about the structure of DMABN in the excited state.

Experimental Section

Materials: All chemicals were purchased from Sigma-Aldrich unless otherwise indicated. *p*-Nitroaniline (>99%) was purified by recrystallization from benzene (Alfa Aesar) before use. Two ^{15}N-substituted isotopomers of PNA were synthesized according to published methods. *p*-(^{15}N)Nitroaniline (PNA-$^{15}NO_2$) was synthesized by nitration[43] of acetanilide (97%) with $K^{15}NO_3$ (98 atom% ^{15}N) and subsequent hydrolysis. The product was recrystallized from ethanol. *p*-Nitro(^{15}N)aniline (PNA-$^{15}NH_2$) was obtained by nitrating (^{15}N)acetanilide (98 atom% ^{15}N) with reagent-grade KNO_3 (>99%) followed by hydrolysis. The product was separated by column chromatography on silica gel, first with *n*-hexane and then with *n*-hexane/ethyl acetate (80/20 v/v) as eluents. The synthesized isotopomers were characterized by ^1H NMR, UV/Vis, and FTIR spectroscopy and mass spectrometry. For UV/Vis and FTIR measurements, [D_3]acetonitrile (99.8 atom% D, Cambridge Isotope Laboratories) was used as solvent. The UV/Vis spectra of PNA-$^{15}NH_2$ and PNA-$^{15}NO_2$ evidenced no noticeable difference from that of normal PNA.

^1H NMR (300 MHz, [D_6]DMSO): $\delta = 7.94$–7.91 (m, 2H), 6.7 (s, 2H), 6.59–6.56 ppm (m, 2H); MS (EI): m/z (%): 139 (100) [M^+]; UV/Vis ([D_3]acetonitrile): λ_{max} (ε) = 364 nm (17830 $mol^{-1}\,dm^3\,cm^{-1}$).

Nanosecond time-resolved dispersive IR spectroscopy: The apparatus for nanosecond time-resolved dispersive IR spectroscopy has been described in detail elsewhere.[34,44] This apparatus utilizes a dispersive monochromator in combination with an alternating current (AC)-coupled detection scheme.[35,45] Because the grating of the spectrometer must be scanned to record a spectrum, the dispersive method usually requires much longer acquisition time than the FTIR method. However, the dispersive method has higher sensitivity of up to $\Delta A \approx 1 \times 10^{-6}$,[44] which is hardly accessible with the FTIR method.[46] Furthermore, the dispersive method is less susceptible to the instability of the measured transient event in comparison with the FTIR method.[46]

The third harmonic of a Q-switched Nd:YAG laser (355 nm; 7 ns duration; 56 μJ energy; 500 Hz repetition rate) was used to photoexcite the sample. The excitation wavelength lies very close to the absorption maximum (364 nm) of PNA in CD_3CN, which corresponds to the $S_1 \leftarrow S_0$ transition. The changes in absorption spectrum upon photoexcitation were probed with mid-IR light derived from a ceramic IR emitter. The probe light transmitted through the 100 μm-thick sample was introduced to a dispersive spectrometer and detected with a photovoltaic HgCdTe detector that was coupled to a preamplifier. The AC-coupled output of the detector was further amplified and finally processed with a high-speed digitizer mounted on a computer, yielding a time stream of IR difference spectra in the fingerprint region (1200–1700 cm^{-1} in the present case). A spectral resolution of 8 cm^{-1} was used. The time resolution of the apparatus was approximately 80 ns, which was determined by the temporal response of the HgCdTe detector to a 7 ns pulse. The concentration of PNA in CD_3CN was kept as low as 0.25 mM, so that depletion of the ground-state absorption almost fully recovers at longer delay times and no long-lived photoproducts of PNA were detected to a measurable extent. To avoid possible sample degradation and heat accumulation due to laser irradiation, the sample solution was continuously circulated by a gear pump through a laboratory-built flow cell consisting of two calcium fluoride windows. In a normal run, the sample solution in the reservoir was continuously bubbled with argon gas, whereas in the oxygen-quenching experiment, it was saturated with oxygen gas. The ground-state IR spectra of PNA and its isotopomers were also recorded on a JASCO FT/IR-6100 spectrometer with a spectral resolution of 2 cm^{-1}. All measurements were performed at room temperature.

Computational details: DFT calculations were performed with the B3LYP functional[47,48] and the cc-pVTZ basis set[49] as implemented in Gaussian 09.[50] Geometry optimization with tight convergence criteria was followed by frequency and IR intensity calculations in a double harmonic approximation, in which both positions and intensities of the bands are determined by retaining only the lowest nonvanishing terms in the Taylor expansions of the potential energy and dipole moment. The lack of anharmonicity in the calculated B3LYP spectra was partially compensated by performing a uniform scaling of the computed frequencies by a factor of 0.972. The polarizable continuum model (PCM) was tested to see the implicit solvation effects on the solute. Calculated IR spectra were plotted using a Gaussian spectral envelope with a half-width at half-maximum of 8 cm^{-1}. In the engineered spectra, we slightly elongated the C–NH_2 distance and performed partial geometry optimization (with the C–NH_2 distance frozen) followed by frequency determination for such a nonequilibrium structure. All vibrational modes are nonimaginary and, differ only slightly (by up to 15 cm^{-1}) from the original spectrum.

Acknowledgements

This work was supported by the "Aiming for the Top University" plan of the Ministry of Education, Taiwan, and National Chiao Tung University. We also acknowledge financial support from the National Science Council of Taiwan (Grants NSC98-2113M-009-011-MY2 to S.S. and NSC99-2113M-009-022-MY3 to H.A.W.).

[1] D. J. Craik, G. C. Levy, R. T. C. Brownlee, *J. Org. Chem.* **1983**, *48*, 1601.
[2] R. R. Fraser, *J. Am. Chem. Soc.* **1982**, *104*, 6475.
[3] H. C. Hiberty, G. Ohanessian, *J. Am. Chem. Soc.* **1984**, *106*, 6963.
[4] A. M. Moran, A. M. Kelley, *J. Chem. Phys.* **2001**, *115*, 912.
[5] S. P. Karna, P. N. Prasad, M. Dupuis, *J. Chem. Phys.* **1991**, *94*, 1171.
[6] C. Castiglioni, M. Del Zoppo, G. Zerbi, *Phys. Rev. B* **1996**, *53*, 13319.
[7] C. Dehu, F. Meyers, E. Hendrickx, K. Clays, A. Persoons, S. R. Marder, J. L. Brédas, *J. Am. Chem. Soc.* **1995**, *117*, 10127.
[8] J. N. Woodford, M. A. Pauley, C. H. Wang, *J. Phys. Chem. A* **1997**, *101*, 1989.
[9] F. L. Huyskens, P. L. Huyskens, A. P. Persoons, *J. Chem. Phys.* **1998**, *108*, 8161.

[10] P.-E. Larsson, L. M. Kristensen, K. V. Mikkelsen, *Int. J. Quantum Chem.* **1999**, *75*, 449.
[11] F. Sim, S. Chin, M. Dupuis, J. E. Rice, *J. Phys. Chem.* **1993**, *97*, 1158.
[12] T. P. Carsey, G. L. Findley, S. P. McGlynn, *J. Am. Chem. Soc.* **1979**, *101*, 4502.
[13] J. Dreyer, V. Kozich, W. Werncke, *J. Chem. Phys.* **2007**, *127*, 234505.
[14] K. Mohanalingam, D. Yokoyama, C. Kato, H. Hamaguchi, *Bull. Chem. Soc. Jpn.* **1999**, *72*, 389.
[15] T. Fujisawa, M. Terazima, Y. Kimura, *J. Phys. Chem. A* **2008**, *112*, 5515.
[16] T. Gunaratne, J. R. Challa, M. C. Simpson, *ChemPhysChem* **2005**, *6*, 1157.
[17] V. Kozich, W. Werncke, J. Dreyer, K.-W. Brzezinka, M. Rini, A. Kummrow, T. Elsaesser, *J. Chem. Phys.* **2002**, *117*, 719.
[18] V. Kozich, W. Werncke, A. I. Vodchits, J. Dreyer, *J. Chem. Phys.* **2003**, *118*, 1808.
[19] K. Kumar, P. R. Carey, *J. Chem. Phys.* **1975**, *63*, 3697.
[20] E. D. Schmid, M. Moschallski, W. L. Peticolas, *J. Phys. Chem.* **1986**, *90*, 2340.
[21] S. Shigeto, H. Hiramatsu, H. Hamaguchi, *J. Phys. Chem. A* **2006**, *110*, 3738.
[22] H. Ma, S. Yao, J. Zhang, C. Pu, S. Zhao, M. Wang, J. Xiong, *J. Photochem. Photobiol. A* **2009**, *202*, 67.
[23] V. Chiş, M. M. Venter, N. Leopold, O. Cozar, *Vib. Spectrosc.* **2008**, *48*, 210.
[24] E. Kavitha, N. Sundaraganesan, S. Sebastian, *Indian J. Pure Appl. Phys.* **2010**, *48*, 20.
[25] D. Kosenkov, L. Slipchenko, *J. Phys. Chem. A* **2011**, *115*, 392.
[26] G. Scalmani, M. J. Frisch, B. Mennucci, J. Tomasi, R. Cammi, V. Barone, *J. Chem. Phys.* **2006**, *124*, 094107.
[27] H. K. Sinha, K. Yates, *Can. J. Chem.* **1991**, *69*, 550.
[28] V. M. Farztdinov, R. Schanz, S. A. Kovalenko, N. P. Ernsting, *J. Phys. Chem. A* **2000**, *104*, 11486.
[29] S. A. Kovalenko, R. Schanz, V. M. Farztdinov, H. Hennig, N. P. Ernsting, *Chem. Phys. Lett.* **2000**, *323*, 312.
[30] W. Schuddeboom, J. M. Warman, H. A. M. Biemans, E. W. Meijer, *J. Phys. Chem.* **1996**, *100*, 12369.
[31] C. L. Thomsen, J. Thøgersen, S. R. Keiding, *J. Phys. Chem. A* **1998**, *102*, 1062.
[32] A. L. McClellan, *Tables of Experimental Dipole Moments*, W. H. Freeman and Company, San Francisco, **1963**.
[33] J. Wolleben, A. C. Testa, *J. Phys. Chem.* **1977**, *81*, 429.
[34] S. Yabumoto, S. Sato, H. Hamaguchi, *Chem. Phys. Lett.* **2005**, *416*, 100.
[35] T. Yuzawa, C. Kato, M. W. George, H. Hamaguchi, *Appl. Spectrosc.* **1994**, *48*, 684.
[36] M. Hashimoto, H. Hamaguchi, *J. Phys. Chem.* **1995**, *99*, 7875.
[37] C. Chudoba, A. Kummrow, J. Dreyer, J. Stenger, E. T. J. Nibbering, T. Elsaesser, K. A. Zachariasse, *Chem. Phys. Lett.* **1999**, *309*, 357.
[38] H. Okamoto, *J. Phys. Chem. A* **2000**, *104*, 4182.
[39] H. Okamoto, H. Inishi, Y. Nakamura, S. Kohtani, R. Nakagaki, *J. Phys. Chem. A* **2001**, *105*, 4182.
[40] C. Ma, W. M. Kwok, P. Matousek, A. W. Parker, D. Phillips, W. T. Toner, M. Towrie, *J. Phys. Chem. A* **2001**, *105*, 4648.
[41] W. M. Kwok, C. Ma, P. Matousek, A. W. Parker, D. Phillips, W. T. Toner, M. Towrie, S. Umapathy, *J. Phys. Chem. A* **2001**, *105*, 984.
[42] Z. R. Grabowski, K. Rotkiewicz, W. Rettig, *Chem. Rev.* **2003**, *103*, 3899.
[43] Z. Cao, K. Armstrong, M. Shaw, E. Petry, N. Harris, *Synthesis* **1998**, 1724.
[44] S. Yabumoto, S. Shigeto, Y.-P. Lee, H. Hamaguchi, *Angew. Chem.* **2010**, *122*, 9387; *Angew. Chem. Int. Ed.* **2010**, *49*, 9201.
[45] K. Iwata, H. Hamaguchi, *Appl. Spectrosc.* **1994**, *48*, 1453.
[46] P. Chen, R. A. Palmer, *Appl. Spectrosc.* **1997**, *51*, 580.
[47] A. D. Becke, *J. Chem. Phys.* **1993**, *98*, 5648.
[48] C. Lee, W. Yang, R. G. Parr, *J. Phys. Rev. B* **1988**, *37*, 785.
[49] T. H. Dunning Jr., *J. Chem. Phys.* **1989**, *90*, 1007.
[50] Gaussian 09 (Revision A.02), M. J. Frisch, G. W. Trucks, H. B. Schlegel, G. E. Scuseria, M. A. Robb, J. R. Cheeseman, G. Scalmani, V. Barone, B. Mennucci, G. A. Petersson, H. Nakatsuji, M. Caricato, X. Li, H. P. Hratchian, A. F. Izmaylov, J. Bloino, G. Zheng, J. L. Sonnenberg, M. Hada, M. Ehara, K. Toyota, R. Fukuda, J. Hasegawa, M. Ishida, T. Nakajima, Y. Honda, O. Kitao, H. Nakai, T. Vreven, J. A. Montgomery, Jr., J. E. Peralta, F. Ogliaro, M. Bearpark, J. J. Heyd, E. Brothers, K. N. Kudin, V. N. Staroverov, R. Kobayashi, J. Normand, K. Raghavachari, A. Rendell, J. C. Burant, S. S. Iyengar, J. Tomasi, M. Cossi, N. Rega, J. M. Millam, M. Klene, J. E. Knox, J. B. Cross, V. Bakken, C. Adamo, J. Jaramillo, R. Gomperts, R. E. Stratmann, O. Yazyev, A. J. Austin, R. Cammi, C. Pomelli, J. W. Ochterski, R. L. Martin, K. Morokuma, V. G. Zakrzewski, G. A. Voth, P. Salvador, J. J. Dannenberg, S. Dapprich, A. D. Daniels, Ö. Farkas, J. B. Foresman, J. V. Ortiz, J. Cioslowski, and D. J. Fox, Gaussian, Inc., Wallingford, CT, **2009**.

Received: October 13, 2011
Published online: January 25, 2012

